ELSEVIER

Chemical Engineering Journal 134 (2007) 16–22

Chemical Engineering Journal

www.elsevier.com/locate/cej

Water–gas shift activity of doped Pt/CeO_2 catalysts

P. Panagiotopoulou [a], J. Papavasiliou [a,b], G. Avgouropoulos [b], T. Ioannides [b], D.I. Kondarides [a,*]

[a] *Department of Chemical Engineering, University of Patras, GR-26504 Patras, Greece*
[b] *Foundation for Research and Technology-Hellas (FORTH), Institute of Chemical Engineering and High Temperature Chemical Processes (ICE-HT), P.O. Box 1414, GR-26504 Patras, Greece*

Abstract

A series of platinum catalysts supported on cation (Me)-doped cerium oxide (Me = Ca, La, Mg, Zn, Zr, Yb, Y, Gd) have been prepared employing the urea-nitrate combustion method. The effects of Me-promotion on the physicochemical and chemisorptive properties of Pt/CeO_2 catalysts and on their catalytic performance for the water–gas shift (WGS) reaction have been investigated. It has been found that the WGS activity of Pt/Ce-Me-O catalysts depends on the nature of the dopant employed, varying in the order of Yb > Gd > Zr > Mg > La > CeO_2(undoped) > Ca > Y > Zn, with the Yb-promoted catalyst being about one order of magnitude more active than the Zn-promoted one, at 250 °C. Evidence is provided that promotion affects the reducibility and oxygen ion mobility of the CeO_2 support, which in turn affects the WGS activity of dispersed platinum crystallites.

Keywords: Water–gas shift; Platinum; Cerium oxide; Doping; Combustion synthesis; FTIR; TPR; Carbon monoxide

1. Introduction

One of the most important components of the fuel processors which are under development for the conversion of hydrocarbon fuels into hydrogen rich gas streams is the water–gas shift (WGS) unit, which serves for both preliminary CO cleanup and additional hydrogen production [1,2]. Conventional low-temperature (Cu/ZnO/Al_2O_3) and high-temperature (Fe_3O_4/Cr_2O_3) WGS catalysts cannot be used in power generation systems for transportation and residential applications due to restrictions related to their volume and weight and also due to the requirements for reduced start-up times, durability under steady state and transient conditions and stability to condensation and poisons [3].

Among the various metal/support combinations investigated for the low-temperature WGS reaction, ceria-supported precious metal catalysts seem to be promising candidates for fuel cell applications [4–6], exhibiting activity comparable to that of conventional Cu/ZnO/Al_2O_3 catalysts [6]. However, most of these materials are not sufficiently stable and progressively deactivate under conditions typical of a reformer outlet [7]. This has been attributed to several factors, including irreversible reduction of the support [7], structural changes and sintering of the metallic phase [4,8], carbon deposition [9] or formation of cerium hydroxycarbonate species [10]. In addition, the activity of fresh Pt/ceria catalysts was found to be not enough to meet the weight and cost constraints found in automotive applications [7]. As a result, efforts are made to further increase catalytic activity and to improve structural stability of ceria-supported noble metal catalysts.

The WGS activity of ceria-supported precious metal catalysts can be enhanced significantly by addition of surface promoters [8,11–13]. This has been attributed to the effects induced by the presence of promoters on the surface properties of ceria [13], including reducibility, oxygen storage capacity and resistance to sintering [12]. It has been also proposed that the role of the promoter is to lower the barrier for oxygen transfer from ceria to the metal [8], thereby facilitating oxidation of adsorbed CO.

In our previous studies [14,15] it was shown that the WGS activity of supported noble metal catalysts depends strongly on the nature and physicochemical characteristics of the support. In particular, it was found that activity of noble metals is significantly improved when supported on "reducible" rather than on "irreducible" metal oxides [15]. It was also shown that the activity of Pt/TiO_2 catalysts depends strongly on the morphological characteristics of the support, i.e., it increases with decrease of

* Corresponding author. Tel.: +30 2610 969527; fax: +30 2610 991527.
E-mail address: dimi@chemeng.upatras.gr (D.I. Kondarides).

1385-8947/$ – see front matter © 2007 Elsevier B.V. All rights reserved.
doi:10.1016/j.cej.2007.03.054

the primary crystallite size of the titania [14]. This behaviour has been attributed to the higher reducibility of small titania crystallites, which may affect either directly (redox properties) or indirectly (population and reactivity of hydroxyl groups) the WGS activity [14,16]. In contrast, the activity of Pt/CeO_2 catalysts did not depend on the crystallite size of the ceria carrier [15].

In the present study, we report on the WGS activity of Pt catalysts supported on cation (Me)-doped cerium oxide (Me = Ca, La, Mg, Zn, Zr, Yb, Y, Gd) prepared by the urea-nitrate combustion method [17]. The catalytic performance of these Pt/Ce-Me-O catalysts is investigated with respect to the dopant-induced alterations on the physicochemical and chemisorptive characteristics of the support.

2. Experimental

2.1. Catalyst preparation and characterization

Metal-promoted cerium oxide supports were synthesized by the urea-nitrates combustion method [17] by mixing the nitrate salt of the promoter [$Me(NO_3)_z{\cdot}XH_2O$] (Me: Yb, Gd, Zr, Mg, La, Ca, Y, Zn) with cerium nitrate [$Ce(NO_3)_3{\cdot}6H_2O$] and urea (CH_4N_2O) in appropriate molar ratios (Me/(Me + Ce) = 0.10, 75% excess of urea). The crucible containing the mixed solution was initially preheated on a hot plate at ∼80 °C, so that excess water was removed. After the solution was converted to a viscous gel, it was placed in an open muffle furnace maintained at 400–500 °C. The gel started boiling and autoignited with rapid evolution of a large quantity of gases, yielding a foamy, voluminous powder, which was further treated at 550 °C for 1 h. Dispersed platinum catalysts were prepared employing the wet impregnation method [14] with the use of the above promoted cerium oxide powders and $(NH_3)_2Pt(NO_2)_2$. After preparation, Pt/Me-Ce-O catalysts were reduced at 300 °C in hydrogen flow for 2 h. In all cases, the platinum loading was 0.5 wt.%.

Materials were characterized with respect to their specific surface area, primary crystallite size of the support and platinum dispersion, employing nitrogen physisorption at the temperature of liquid nitrogen (BET method), X-ray diffraction (XRD) and selective chemisorption of CO, respectively [14]. Platinum dispersion, expressed in terms of CO/Pt ratio, was estimated assuming that each Pt metal atom chemisorbs one CO molecule. Temperature-programmed reduction (TPR) experiments were performed under a flow of a 3% H_2/He mixture (50 $cm^3\ min^{-1}$) over 200 mg of preoxidized catalyst using a heating rate of 10 °C min^{-1}. A mass spectrometer (Omnistar/Pfeiffer Vacuum) was used for on-line monitoring of TPR effluent gas. FTIR experiments were carried out using a Nicolet 740 FTIR spectrometer equipped with a DRIFT cell, an MCT detector and a KBr beam splitter [18], following the procedures described in detail elsewhere [16,18].

The catalytic performance of Pt/Ce-Me-O catalysts for the WGS reaction was investigated in the temperature range of 100–550 °C using a feed stream consisting of 3%CO and 10%H_2O (balance: He). In a typical experiment, 75 mg of the catalyst powder (particle size: $0.18 < d < 0.25$ mm) are placed in a quartz microreactor and reduced *in situ* at 300 °C for 1 h under a hydrogen flow of 60 $cm^3\ min^{-1}$. The catalyst is then heated at 500 °C under He flow and left at that temperature for 15 min. Finally, the catalyst is conditioned at 450 °C for 1 h, under the flowing reaction mixture (total flow: 150 $cm^3\ min^{-1}$). Measurements of intrinsic rates were obtained under differential reaction conditions. Results were used to determine the turnover frequencies (TOFs) of carbon monoxide consumption, defined as moles of CO converted per surface noble metal atom per second. Details of the techniques and procedures employed can be found elsewhere [14–16].

3. Results

3.1. Catalyst characterization

Results of catalyst characterization measurements are summarized in Table 1. It is observed that doping of the support generally results in a substantial increase of the BET surface area, which increases from 8 $m^2\ g^{-1}$ for the undoped Pt/CeO_2 catalyst to 20–50 $m^2\ g^{-1}$ for the Pt/Ce-Me-O samples. This is accompanied by a parallel decrease of the primary crystallite size of ceria (d_{CeO_2}) from 18.5 to 7.9–15.5 nm, respectively. The dispersion of platinum varies between 40 and 60%, with the exception of La- and Zr-doped samples, where Pt dispersion is higher.

Table 1
Results of catalyst characterization and of kinetic measurements obtained from the investigated 0.5%Pt/(Ce-Me-O) catalysts

Promoter (Me)	S_{BET} ($m^2\ g^{-1}$)	d_{CeO_2} [a] (nm)	Pt dispersion (%)	Rate at 250 °C (μmol $s^{-1}\ g^{-1}$)	TOF at 250 °C (s^{-1})	Activation energy (kcal mol^{-1})
Yb	41	7.9	40	13.10	1.28	18.8
Gd	42	9.4	52	11.10	0.83	20.5
Zr	27	11.0	100	10.70	0.42	19.9
Mg	33	10.2	58	10.10	0.68	20.4
La	50	8.9	73	9.65	0.52	19.2
Ca	43	8.0	45	6.22	0.54	20.9
Y	28	11.2	48	5.21	0.42	20.5
Zn	20	15.5	37	1.33	0.14	20.0
Undoped	8	18.5	46	6.53	0.55	18.2

[a] Primary particle size of CeO_2 determined by XRD line broadening of the (3 1 1) peak.

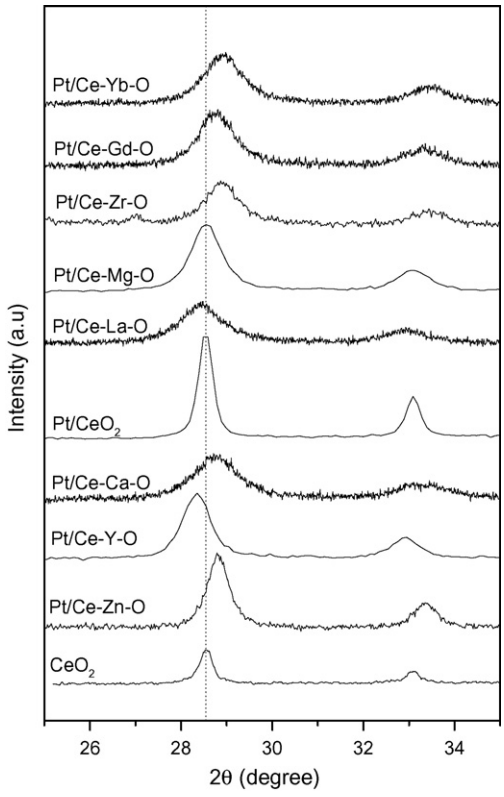

Fig. 1. XRD profiles of the investigated Pt/Ce-Me-O catalysts.

XRD patterns obtained from the Pt/Ce-Me-O catalysts are shown in Fig. 1. Diffraction patterns obtained from undoped Pt/CeO_2 and from unplatinized CeO_2 samples prepared by the same method are also shown for comparison. Results show that CeO_2 obtained by the urea-nitrate method has the typical fluorite-type oxide structure. The lattice constant of the cubic cell of ceria, calculated from the (3 1 1) crystallographic plane, is found to be equal to 5.4118 Å (Table 2), in agreement with previous studies [19]. Taking into account the observed shift of the diffraction peaks of ceria in the doped samples (Fig. 1), it can be argued that the added cations with ionic radii [20] different than that of Ce^{4+} are incorporated in the ceria lattice. Incorporation into the ceria lattice of a cation with a smaller ionic radius than that of Ce^{4+}, e.g. Zn^{2+}, Mg^{2+}, Zr^{4+}, results in a decrease of the lattice constant (Table 2) and in a shift of the XRD peaks towards higher diffraction angles (Fig. 1). On the other hand, La^{3+} and Y^{3+}, which have a bigger ionic radius than that of Ce^{4+}, shift the diffraction peaks to lower diffraction angles and the La^{3+}- and Y^{3+}-doped ceria have bigger lattice constant (Table 2). Yb^{3+} and Gd^{3+}, which also have bigger ionic radii, do not induce the same affect on the lattice parameter. This can be explained by the great solubility and by the complex lattice parameter dependencies which have been reported between Gd_2O_3, Yb_2O_3 and CeO_2 [21]. Although the ionic radius of Ca^{2+} (1.12 Å) is similar to that of La^{3+} (1.16 Å), the Ca-doped sample neither has a greater lattice constant (Table 2) nor it shifts the XRD peaks to smaller degrees (Fig. 1), as La^{3+} does. On the contrary, it has the opposite effect. A possible explanation is that the low number of electrons of Ca^{2+} might have provoked some kind of matrix effect, which affects the real lattice constant so that the calculated one is plasmatic.

Table 2
Ceria lattice constants of doped Pt/Ce-Me-O catalysts

Catalyst	Cation	Ionic radius (Å)	Lattice constant, a[a] (Å)
CeO_2	Ce^{4+}	0.970	5.411_8
Pt/CeO_2	Ce^{4+}	0.970	5.411_8
Pt/Ce-La-O	La^{3+}	1.160	5.440_3
Pt/Ce-Mg-O	Mg^{2+}	0.890	5.405_7
Pt/Ce-Zr-O	Zr^{4+}	0.840	5.363_1
Pt/Ce-Zn-O	Zn^{2+}	0.900	5.384_6
Pt/Ce-Ca-O	Ca^{2+}	1.120	5.391_4
Pt/Ce-Y-O	Y^{3+}	1.019	5.421_1
Pt/Ce-Yb-O	Yb^{3+}	0.985	5.370_8
Pt/Ce-Gd-O	Gd^{3+}	1.053	5.394_7

[a] Calculated from the (3 1 1) crystallographic plane

3.2. Temperature-programmed reduction with H_2

Hydrogen consumption curves obtained from the preoxidized Pt/Ce-Me-O catalyst samples are shown in Fig. 2. The TPR profile of the unplatinized CeO_2 sample, which is shown for comparison, is characterized by a broad, high-temperature (HT) feature, which appears above 600 °C and is assigned to reduction of ceria [22,23]. In addition to the HT feature, the TPR profiles of Pt/Ce-Me-O catalysts are characterized by a low-temperature (LT) peak (<150 °C) and two medium temperature (MT) features located at ca. 200 °C (MT1) and ca. 400 °C

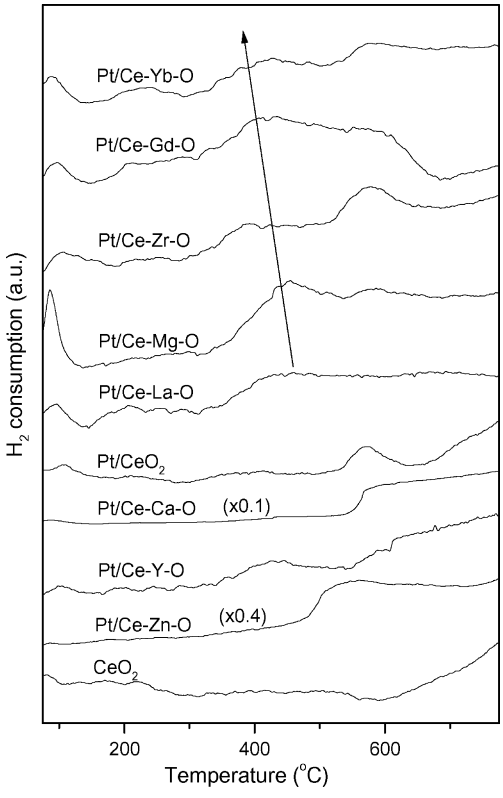

Fig. 2. TPR profiles of Pt/Ce-Me-O catalysts.

(MT2), respectively (Fig. 2). The LT consumption peak, which is observed for all Pt-containing samples investigated (Fig. 2), is attributed to reduction of PtO_x species formed during the pre-oxidation step [16,24]. The MT2 peak at ca. 400 °C is attributed to the Pt-catalyzed reduction of the surface cell of ceria [5,22]. The exact position of this TPR feature depends on the nature of the dopant cation employed and, as will be discussed below, may be connected to the WGS activity of Pt/Ce-Me-O catalysts. Finally, the MT1 feature at around 200 °C, which appears over most doped samples may be tentatively attributed to reduction of ceria in the vicinity of Pt crystallites.

3.3. WGS activity of Pt/Ce-Me-O catalysts

Results of catalytic performance tests obtained over the Pt/Ce-Me-O catalysts are presented in Fig. 3, where the conversion of CO (X_{CO}) is plotted as a function of reaction temperature. The equilibrium conversion, predicted by thermodynamics, is also shown for comparison. It is observed that doping of Pt/ceria with Ca (line 3), Gd, Mg, La (line 2) and, especially, Yb (line 1) results in a shift of the conversion curves toward lower reaction temperatures, compared to the one of the unpromoted catalyst (line 4). Similar was the effect of addition of Zr, which gave a conversion curve located between lines 1 and 3 (not shown for clarity). In contrast, doping with Y (line 5) and, especially, Zn (line 6) results in a decrease of catalytic activity, which is much more pronounced for the latter sample. The catalyst promoted with Yb, which exhibits superior catalytic performance, compared to the other samples, becomes active at temperatures higher than 170 °C and X_{CO} reaches equilibrium conversions at temperatures around 320 °C.

Measurements of intrinsic reaction rates were obtained in separate experiments under differential reaction conditions and results are summarized in Table 1. It is observed that the specific reaction rate (per gram of catalyst) at 250 °C depends strongly on the nature of the promoter used, following the order of Yb > Gd > Zr > Mg > La > CeO_2(undoped) > Ca > Y > Zn, with the rate for the Yb-promoted catalyst being about one order of magnitude higher than that for the Zn-promoted sample. The apparent activation energy (E_a) of the reaction has been calculated for each catalyst from the slope of the Arrhenius plot of reaction rates obtained in the temperature range of 180–280 °C and results are summarized in Table 1. It is observed that E_a does not vary significantly from one catalyst to another, taking values between 18 and 21 kcal mol^{-1} for all samples investigated. This implies that, under the present experimental conditions, the rate-limiting step is not affected by the presence of the promoters investigated. The calculated values of activation energy are in agreement with those reported previously for CeO_2-supported Pt, Rh, Pd and Ru catalysts ([15] and refs. therein).

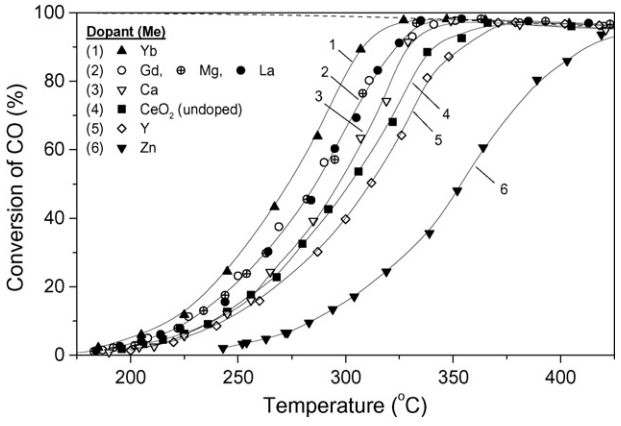

Fig. 3. Catalytic performance of the indicated Pt/Ce-Me-O catalysts for the WGS reaction. Equilibrium conversion of CO is shown with dashed line.

3.4. FTIR investigation of CO adsorption over selected Pt/Ce-Me-O catalysts

Results presented in Fig. 3 and Table 1 clearly show that, among the various samples investigated, the Yb-doped and the Zn-doped catalysts exhibit the best and the worst WGS activity, respectively. Therefore, these samples, along with the undoped Pt/CeO_2 catalyst were further investigated by DRIFT spectroscopy in order to study the effects of doping on the nature and thermal stability of adsorbed CO species. FTIR spectra obtained from the prereduced catalysts following interaction with 1%CO/He at 25 °C for 30 min and subsequent purging with He for 10 min are shown in Fig. 4. It is observed that the spectrum for the undoped Pt/CeO_2 catalyst (trace a) is characterized by three bands in the ν(CO) stretching frequency region, located at 2085, 2068 and 1820 cm^{-1}, and by several bands located below

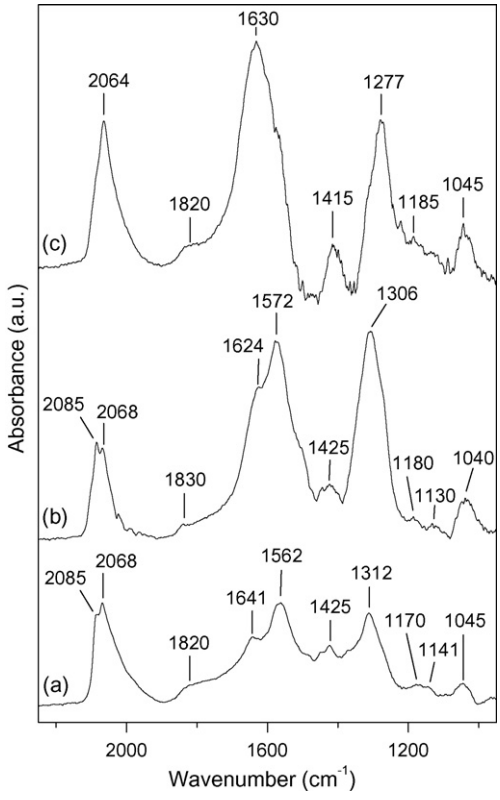

Fig. 4. DRIFT spectra obtained at 25 °C from: (a) Pt/CeO_2(undoped), (b) Pt/Ce-Zn-O and (c) Pt/Ce-Yb-O catalysts following exposure to 1%CO/He for 30 min at 25 °C.

1650 cm^{-1}. The bands at 2085 and 2068 cm^{-1}, are due to CO linearly adsorbed on partially oxidized ($Pt^{\delta+}$) and reduced (Pt^0) platinum sites, respectively, while the band at ca. 1820 cm^{-1} is characteristic of bridge-bonded CO on Pt^0 sites [16,25–28]. Bands located at 1641, 1562, 1425, 1312, 1170 and 1045 cm^{-1} are attributable to surface formate and/or carbonate species associated with the support [27–31]. Qualitatively similar spectra were obtained from the Zn-doped (trace b) and the Yb-doped samples (trace c). The main difference is that the relative intensities of the bands located below 1650 cm^{-1}, compared to those in the ν(CO) region, are higher over the doped catalysts, which is due to the higher surface area of the latter samples (Table 1).

Fig. 5 shows the FTIR spectra in the ν(CO) region obtained from the prereduced Pt/CeO_2, Pt/Ce-Zn-O and Pt/Ce-Yb-O catalysts following adsorption of CO at 25 °C and subsequent stepwise heating at 450 °C under He flow. In the case of unpromoted Pt/CeO_2 catalyst (Fig. 5A), increasing temperature from 25 to 100 °C (traces a–c) results in the disappearance of the bands corresponding to CO adsorbed on $Pt^{\delta+}$ sites (2085 cm^{-1}) and bridge-bonded CO (1820 cm^{-1}). The band at 2068 cm^{-1}, attributed to linearly adsorbed CO on Pt^0 sites, is thermally more stable and disappears from the spectrum at temperatures higher than 200 °C (traces f and g). This is accompanied by a progressive shift of the peaks' maximum from 2068 to 2050 cm^{-1}, which is consistent with a decrease in the dipole–dipole coupling effect between adsorbed CO molecules with decreasing coverage [25,26,32,33].

Two additional bands, located at ca. 1980 and 1750 cm^{-1} become discernible at temperature higher than 75 °C and are present in the spectra at temperatures up to 150 °C (traces b–e). The former band appears at vibrational frequencies lower than those expected for Pt^0–CO species, which indicates the presence of adsorption sites of exceptional electron-donating power. In accordance with previous studies over Pt/CeO_2 [27] and Pd/CeO_2 [34] catalysts, the 1980 cm^{-1} band may be assigned to CO adsorbed on platinum atoms interacting with Ce^{3+} ions of the support. Similar low frequency bands have been also reported for CO adsorbed on TiO_2-supported noble metal catalysts, including Pt/TiO_2 [16,33] and Au/TiO_2 [35] and have been attributed to CO adsorption at metal–Ti^{3+} sites located at the metal/support interface.

The band at ca. 1750 cm^{-1} has been previously assigned to a tilted CO species, adsorbed through both the carbon and oxygen ends [27]. Yee et al. [27] reported that the presence of tilted CO species indicates involvement of the support, which is manifested by partial encapsulation of platinum by the partially reduced ceria. The authors proposed that Ce cations influence the adsorption state of CO by enhancing the back-bonding through the metal. Similar bands, attributed to tilted CO species, have been also observed at 1704 cm^{-1} for 1.6%Rh–1.9%Nb/SiO_2 [36], at 1731 cm^{-1} for Pd/CeO_2 [37], and at 1660 cm^{-1} for Rh/ZrO_2 catalyst [38]. The presence of the bands located at 1980 and 1750 cm^{-1} provides evidence for the involvement of metal/support interactions in the adsorption of CO on the present catalyst [27,37,38].

FTIR spectra obtained from the less active Zn-doped catalyst are shown in Fig. 5B. Comparison with the corresponding spectra obtained from the undoped sample (Fig. 5A) shows the following differences: (a) bands attributed to CO adsorbed on $Pt^{\delta+}$ sites, i.e., at wavenumbers higher than ca. 2080 cm^{-1}, are present in the spectra at temperatures as high as 150 °C (traces a–d); (b) a band located at ca. 2024 cm^{-1} is observed in the tem-

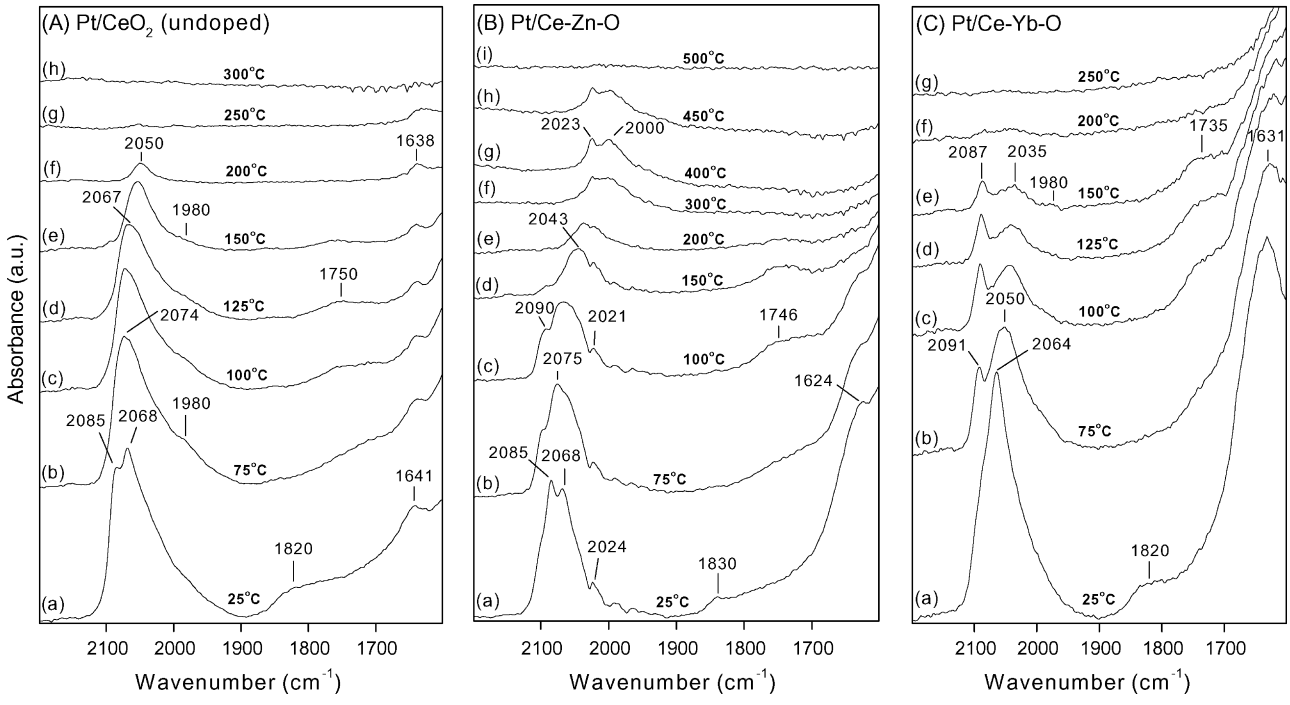

Fig. 5. DRIFT spectra obtained from: (A) Pt/CeO_2(undoped), (B) Pt/Ce-Zn-O and (C) Pt/Ce-Yb-O catalysts following CO desorption at 25 °C and subsequent stepwise heating under He flow.

perature range of 25–450 °C. This band, which does not shift with increase of temperature, may be attributed to linear CO adsorbed on isolated Pt sites; (c) the band attributed to Pt^0–CO species shifts from 2068 to ca. 2000 cm^{-1} with increase of temperature from ca. 25 to 450 °C cm^{-1} (traces a–h). Interestingly, the temperature required to eliminate this peak from the spectrum (450–500 °C) is much higher than that required for the undoped sample (200–250 °C) (Fig. 5A). This clearly shows that doping of Pt/CeO_2 with Zn results in a significant enhancement of the thermal stability of the adsorbed CO species.

The corresponding spectra obtained from the highly active Pt/Ce-Yb-O catalyst are shown in Fig. 5C. It is observed that, as in the case of the Zn-doped catalyst (Fig. 5B), bands attributable to $Pt^{\delta+}$–CO, located at ca. 2090 cm^{-1}, can be clearly distinguished at temperatures in the range of 75–150 °C (traces b–e). This indicates that the presence of both dopants results in the creation and stabilization of partially oxidized platinum sites. The most interesting observation is that bands due to adsorbed CO disappear from the spectra at temperatures below 250 °C, i.e., lower than those observed for the undoped Pt/CeO_2 catalyst.

4. Discussion

Results of XRD experiments summarized in Fig. 1 and Table 2 show that addition of promoters shifts the diffraction peaks and affects the lattice parameters of ceria in a manner which depends on the ionic radius of the dopant cation. It may then be argued that the added cations are incorporated into the ceria lattice. Substitution of the tetravalent Ce^{4+} cation by divalent, trivalent or tetravalent cations results in the creation of oxygen vacancies, which can be directly related to the WGS activity [39,40].

Catalytic performance tests (Fig. 3) and kinetic measurements (Table 1) clearly show that doping of ceria affects strongly the WGS activity of supported Pt catalysts. This cannot be attributed to variations of Pt dispersion which, with the exception of Zr- and La-promoted samples, does not vary significantly for the catalysts investigated (Table 1). Therefore, the observed differences in the catalytic activity of the Pt/Ce-Me-O catalysts should be attributed to differences in the physicochemical properties of the support. This is in accordance with our previous investigations where it was found that the specific reaction rate (TOF) does not depend on metal loading, dispersion or crystallite size for Pt/CeO_2, Pt/TiO_2, Ru/TiO_2 and Pt/Al_2O_3 catalysts [14,15]. Results summarized in Table 1 also demonstrate that there is no direct relation between the specific surface area (or d_{CeO_2}) of the investigated catalysts and their WGS activity. Although the surface area of the promoted samples is substantially higher than that of undoped Pt/CeO_2, there are not significant differences between the surface areas of the doped Pt/Ce-Me-O samples. It may then be concluded that the effect of promotion on the WGS activity of the present catalysts is of chemical nature and is not related to the morphological or structural characteristics of the support.

TPR profiles of Fig. 2 indicate that a relation may exist between the WGS activity of Pt/Ce-Me-O catalysts and their reduction characteristics (note that curves shown, from bottom to top, are plotted in the order of increasing WGS activity). It is observed that, as a general trend, the lower the temperature of the MT2 peak, attributed to reduction of the surface cell of ceria, the higher the WGS activity. In contrast, catalysts which are less active than undoped Pt/CeO_2 either do not exhibit a clear MT2 hydrogen consumption peak (e.g. Ca- and Zn-doped samples) or it appears at higher temperatures (e.g. Y-doped sample). It may then be argued that the catalytic performance of dispersed Pt crystallites for the title reaction depends on the reducibility of the support: the higher the reducibility of surface cell of ceria, the higher the WGS activity of the Pt/Ce-Me-O catalyst.

FTIR results of Fig. 5 show that CO species adsorbed on platinum are thermally more stable over the less active Pt/Ce-Zn-O catalyst (Fig. 5B), compared to the undoped Pt/CeO_2 sample (Fig. 5A). In contrast, FTIR bands disappear at substantially lower temperatures over the highly active Pt/Ce-Yb-O catalyst (Fig. 5C). The observed differences in the temperature required for the disappearance of the bands in the ν(CO) region cannot be solely attributed to dopant-induced alterations in the chemisorptive properties of dispersed Pt crystallites. However, they could be explained by taking into account the competition between the CO desorption process and the possible surface reactions which may take place upon heating. In accordance with the results of our previous investigations over Rh/CeO_2 catalysts [41,42], the disappearance of the IR bands may be attributed to reaction of adsorbed CO with oxygen originating from the support. If this is the case, it may be argued that the low thermal stability of the adsorbed CO species observed for the undoped Pt/CeO_2 (Fig. 5A) and for the Yb-doped (Fig. 5C) samples may be due to the relatively high ability of the corresponding supports to provide active oxygen species, which react with adsorbed CO to yield CO_2 in the gas phase. In contrast, the high thermal stability of CO species adsorbed on Pt/Ce-Zn-O (Fig. 5B) may reflect the comparably lower availability of mobile oxygen atoms of the support. This hypothesis is supported by the TPR results of Fig. 2, which show that the reducibility of the ceria surface is considerably higher than that of the undoped Pt/CeO_2 and, especially, of the Zn-doped sample.

Concluding, it may be suggested that doping of Pt/CeO_2 catalysts with the investigated promoters affects strongly the reducibility characteristics of the support which in turn affects the WGS activity. As a general trend, the WGS activity increases with increasing the reducibility of the surface cell of ceria. This is in accordance with the results of Wang and Gorte [11], who investigated the effect of addition of various promoters on the WGS activity of Pd/CeO_2 catalysts and found significantly enhanced rates for the Fe-promoted sample. They proposed that the role of the promoter is to lower the barrier for oxygen transfer from ceria to the metal, thereby affecting oxygen ion mobility (and reducibility) of the support. It is also in general agreement with our previous findings that the WGS activity of noble metals is significantly improved when supported on reducible metal oxides [14–16].

It should be noted that both the ceria-mediated redox mechanism [4,8] and the formate (associative) reaction mechanism [29,43] may be employed to explain the observed enhancement of WGS activity with increasing the reducibility of the ceria-

based support. According to the redox mechanism, Ce^{4+} cations are reduced toward Ce^{3+} by CO adsorbed on the metal to produce CO_2, while the created oxygen vacancies are replenished by H_2O to produce H_2 [4]. According to the formate mechanism, reduction of ceria results in the formation of the WGS-active bridging OH groups at Ce^{3+} defect sites [29,43]. Whatever the mechanism of the reaction, the rate is expected to increase if Ce^{3+} atoms (i.e., oxygen vacancies) are formed at lower temperatures. Results of the present study show that the temperature required for the reduction of the surface shell of ceria may be reduced and therefore the WGS activity may be increased by doping of Pt/CeO_2 catalysts with appropriate promoters, including La, Mg, Zr, Gd and, especially, Yb.

5. Conclusions

The urea-nitrates combustion method can be used for the preparation of cation (Me)-doped cerium dioxide carriers (Me = Ca, La, Mg, Zn, Zr, Yb, Y, Gd) in which the dopant cations are incorporated into the ceria lattice. The presence of the dopant affects the physicochemical characteristics (e.g. surface area and reducibility) of the support, the chemisorptive properties toward CO, and the WGS activity of Pt/Ce-Me-O catalysts, in a manner which depends on the nature of the dopant cation. Evidence is provided that the WGS activity of dispersed platinum depends on the reducibility of the support or, equivalently, on the mobility and reactivity of surface oxygen atoms of doped ceria. In particular, activity is enhanced with increasing reducibility of the surface cell of ceria, with the rate over the most active Yb-doped catalyst being more than one order of magnitude higher than that of the less active Zn-doped sample.

References

[1] D.L. Trimm, Z.I. Önsan, Catal. Rev. 43 (2001) 31.
[2] A.F. Ghenciu, Curr. Opin. Solid State Mater. Sci. 6 (2002) 389.
[3] J.M. Zalc, D.G. Löffler, J. Power Sources 111 (2002) 58.
[4] T. Bunluesin, R.J. Gorte, G.W. Graham, Appl. Catal. B 15 (1998) 107.
[5] Y. Li, Q. Fu, M. Flytzani-Stephanopoulos, Appl. Catal. B 27 (2000) 179.
[6] Q. Fu, H. Saltsburg, M. Flytzani-Stephanopoulos, Science 301 (2003) 935.
[7] J.M. Zalc, V. Sokolovskii, D.G. Löffler, J. Catal. 206 (2002) 169.
[8] X. Wang, R.J. Gorte, J.P. Wagner, J. Catal. 212 (2002) 225.
[9] A. Goguet, F. Meunier, J.P. Breen, R. Burch, M.I. Petch, A.F. Chenciu, J. Catal. 226 (2004) 382.
[10] Q. Fu, W. Deng, H. Saltsburg, M. Flytzani-Stephanopoulos, Appl. Catal. B 56 (2005) 57.
[11] X. Wang, R.J. Gorte, Appl. Catal. A 247 (2003) 157.
[12] L. Kundakovic, M. Flytzani-Stephanopoulos, Appl. Catal. A 171 (1998) 13.
[13] X. Qi, M. Flytzani-Stephanopoulos, Ind. Eng. Chem. Res. 43 (2004) 3055.
[14] P. Panagiotopoulou, D.I. Kondarides, J. Catal. 225 (2004) 327.
[15] P. Panagiotopoulou, D.I. Kondarides, Catal. Today 112 (2006) 49.
[16] P. Panagiotopoulou, A. Christodoulakis, D.I. Kondarides, S. Boghosian, J. Catal. 240 (2006) 114.
[17] G. Avgouropoulos, T. Ioannides, Appl. Catal. A 244 (2003) 155.
[18] T. Chafik, D.I. Kondarides, X.E. Verykios, J. Catal. 190 (2000) 446.
[19] Y. Liu, T. Hayakawa, T. Tsunoda, K. Suzuki, S. Hamakawa, K. Murata, R. Shiozaki, T. Ishii, M. Kumagai, Top. Catal. 22 (2003) 205.
[20] http://abulafia.mt.ic.ac.uk.
[21] T.H. Etsell, S.N. Flengas, Chem. Rev. 70 (1970) 339.
[22] H.C. Yao, Y.F.Y. Yao, J. Catal. 86 (1984) 254.
[23] G.L. Markaryan, L.N. Ikryannikova, G.P. Muravieva, A.O. Turakulova, B.G. Kostyuk, E.V. Lunina, V.V. Lunin, E. Zhilinskaya, A. Aboukais, Colloids Surf. A 151 (1999) 435.
[24] C.-P. Hwang, C.-T. Yeh, J. Mol. Catal. A 112 (1996) 295.
[25] M. Primet, J. Catal. 88 (1984) 273.
[26] P.-A. Carlsson, L. Österlund, P. Thormählen, A. Palmqvist, E. Fridell, J. Jansson, M. Skoglundh, J. Catal. 226 (2004) 422.
[27] A. Yee, S.J. Morrison, H. Idriss, J. Catal. 191 (2000) 30.
[28] O. Pozdnyakova, D. Tescher, A. Wootsch, J. Kröhnert, B. Steinhauer, H. Sauer, L. Toth, F.C. Jentoft, A. Knop-Gericke, Z. Paál, R. Schlögl, J. Catal. 237 (2006) 1.
[29] T. Shido, Y. Iwasawa, J. Catal. 141 (1993) 71.
[30] T. Shido, Y. Iwasava, J. Catal. 136 (1992) 493.
[31] C. Binet, M. Daturi, J.-C. Lavalley, Catal. Today 50 (1999) 207.
[32] M. Primet, J.M. Basset, M.V. Mathieu, M. Prettre, J. Catal. 29 (1973) 213.
[33] O.S. Alexeev, S.Y. Chin, M.H. Engelhard, L. Ortiz-Soto, M.D. Amiridis, J. Phys. Chem. B 109 (2005) 23430.
[34] A. Bensalem, J.C. Muller, D. Tessier, F. Bozon-Verduraz, J. Chem. Soc. Faraday Trans. 92 (1996) 3233.
[35] F. Boccuzzi, A. Chiorino, M. Manzoli, D. Andreeva, T. Tabakova, J. Catal. 188 (1999) 176.
[36] O.S. Alekseev, T. Beutel, E.A. Paukshtis, Y.A. Ryndin, V.A. Likholobov, H. Knozinger, J. Mol. Catal. 92 (1994) 217.
[37] C. Binet, A. Jadi, J.C. Lavalley, M. Boutonnet-Kizling, J. Chem. Soc. Faraday Trans. 88 (1992) 2079.
[38] E. Guglielminotti, J. Catal. 120 (1989) 287.
[39] S.Y. Choung, M. Ferrandon, T. Krause, Catal. Today 99 (2005) 257.
[40] R. Pérez-Hernádez, F. Aguilar, A. Gómez-Cortés, G. Díaz, Catal. Today 107–108 (2005) 175.
[41] D.I. Kondarides, X.E. Verykios, J. Catal. 174 (1998) 52.
[42] D.I. Kondarides, Z. Zhang, X.E. Verykios, J. Catal. 176 (1998) 536.
[43] S. Ricote, G. Jacobs, M. Milling, Y. Ji, P.M. Patterson, B.H. Davis, Appl. Catal. A 303 (2006) 35.